Colloidal Photonic Crystal Pigments with Low Angle Dependence

Carlos I. Aguirre,[†] Edilso Reguera,[†] and Andreas Stein*[,‡]

CICATA—Legaria IPN, Calz. Legaria # 694, Col. Irrigación, Del. Miguel Hidalgo, C.P. 11500, D.F., México, and Department of Chemistry, University of Minnesota, 207 Pleasant St. SE, Minneapolis, Minnesota 55455, United States

ABSTRACT Poly(methyl methacrylate) (PMMA)-based colloidal photonic crystals have an incomplete photonic band gap (PBG) and typically appear iridescent in the visible range. As powders, synthetic PMMA opals are white, but when infiltrated with carbon black nanoparticles, they exhibit a well-defined color that shows little dependence on the viewing angle. The quantity of black pigment determines the lightness of the color by controlling scattering. The combined effects of internal order within each particle and random orientation among the particles in the powder are responsible for this behavior. These pigments were employed as paints, using a mixture of polyvinyl acetate as a binder and deionized water as the solvent, and were applied to wood and paper surfaces for color analysis.

KEYWORDS: colloidal photonic crystals • synthetic opals • powder pigments • structural color

INTRODUCTION

Iridescence, i.e., angle-dependent, structural color, is one of the defining features of opals and inverse opal photonic crystals in the visible range. These materials have periodic structures in three dimensions, with a periodicity whose length scale is proportional to the wavelength of visible light. The color in opals and inverse opals is due to stop bands or incomplete photonic band gaps (PBGs) that result from multiple scattering and diffraction of light by the ordered structures (1−5). Structural color is particularly vivid in three-dimensionally ordered macroporous (3DOM) oxides with a relatively high refractive index (e.g., 3DOM ZrO_2 and 3DOM TiO_2), which rely on incomplete PBGs for the color effect (6−8). The color of these materials can be tailored by infiltration with solvents of different refractive indices, opening opportunities for new kinds of pigments. Similarly, photonic supraparticles composed of colloidal sphere arrays can exhibit striking opalescent colors (9−11). Several patents mention the use of opals as pigments infiltrated with different materials (12−14). For sufficiently large ordered domains of colloidal photonic crystals, multiple colors (i.e., iridescence) can typically be observed, depending on the viewing angle with respect to given photonic crystal planes. However, there are clues pointing at the possibility of obtaining more definite colors (without iridescence) from these kinds of structures. For example, Takeoka and coworkers developed a hydrogel membrane with 2−4 wt % of a polymer, which displayed a constant color over a viewing angle of 40° (15). Furthermore, the angle dependence of the color of silica sphere arrays could be largely eliminated by adding a second population of smaller spheres, thereby forming amorphous colloidal arrays (16).

Poly(methyl methacrylate) (PMMA) latex spheres have been widely used to fabricate synthetic opals and extended colorful opalescent films (17). However, as powders, such polymeric opals are white, sometimes with some brilliant colorful sparks. On the opposite scale is carbon black, a colloidal form of graphitic carbon and an important black pigment (18). The literature provides evidence that carbon nanoparticles can be used for enhancement of structural color. Pursiainen et al. reported that sub-50-nm carbon nanoparticles, which were uniformly incorporated in the interstices of highly ordered polymeric colloidal crystal films, enhanced the color of these elastomeric films (19). Wang and coworkers observed an enhancement of interference colors after applying a thin carbon layer onto an anodic aluminum oxide film with nanochannels (20). The appearance of pearlescent pigments can also be enhanced by carbon nanoparticles (21).

By mixing white and black powders, one might not necessarily expect to obtain color, but as this study shows, the dark background provided by carbon nanoparticles in contact with opaline domains produces distinctively colored pigments. In this report, the effects of carbon nanoparticles on structural colors of PMMA opals and the dependence of coloration on sphere size, carbon content, viewing angle, and paint vehicles are analyzed. On the basis of structural and spectral analysis of these samples, a qualitative model is proposed to explain the color enhancement and the low degree of angular dependence of the colors of these composite materials.

EXPERIMENTAL SECTION

Methyl methacrylate (99%, Aldrich) and 2,2′-azobis(2-methylpropionamidine) dihydrochloride (97%, Aldrich) were used for the preparation of PMMA spheres of different sizes (340 ± 10 nm, 322 ± 10 nm, 310 ± 10 nm, 270 ± 10 nm, 240 ± 10

* Corresponding author. Tel.: +1-612-624-1802. Fax: +1-612-626-7541. E-mail: a-stein@umn.edu.

Received for review August 6, 2010 and accepted September 27, 2010

[†] CICATA—Legaria IPN.

[‡] University of Minnesota.

DOI: 10.1021/am100704f

nm diameters) by a method reported elsewhere (8). Deionized and charcoal-treated water (18.2 MΩ · cm specific resistance) was used for all sample solutions. PMMA arrays were prepared by centrifugation of aqueous dispersions of colloidal PMMA at 2000 rpm overnight. After decanting of the solvent and drying of the products at room temperature, white monolithic or powdered products of the PMMA colloidal crystals were obtained.

Mixtures of PMMA synthetic opal powder with different amounts of carbon black powder (acetylene black, Chevron Phillips Chemical Company) were prepared by mixing the dry components, crushing the mixture in a porcelain mortar, and sieving it through a 200-mesh sieve to produce particles with dimensions <75 μm. The procedure was repeated for several samples with different sphere sizes. For preparing paint layers, the colored powders were suspended in a solution containing deionized water and polyvinyl acetate glue as a binder ("carpenter's glue", 32 wt % PVA in water, Henkel Mexicana S.A. de C.V.). This paint had a solids concentration of 0.2 % m/v (total solid mass over total volume of water), and the mass ratio of colored powder to PVA was 1:1.

Optical properties of the samples were analyzed using a UV−vis spectrophotometer with a fiber-optic probe (Ocean Optics, model Jaz) and associated Spectra Suite software. Spectra were obtained for randomly oriented bulk powder samples at a normal incidence to the powder surface. Exposed photographic paper was used for a dark reference. The setup for analysis of the paints is described in the Results and Discussion section. SEM images were obtained using JEOL 6500 and JEOL JSM-6390LV scanning electronic microscopes, using samples coated with ca. 5 nm of gold. Particle diameters were estimated from the SEM images. Photographs were taken with a Nikon Coolpix S220 digital camera with flash.

RESULTS AND DISCUSSION

Usually, uncontrolled defects are undesirable in photonic crystals, and among different methods for preparing crystalline arrays of colloids (22), centrifugation is not the best technique for fabricating high quality colloidal photonic crystals. However, it is a relatively rapid and easy method, and while the resulting opals do not have the highest perfection, their periodicity is sufficient to produce an incomplete PBG for our aims. As-prepared PMMA colloidal crystal powders were white (Figure 1a). In contrast, ground mixtures of PMMA opals with only little wt % carbon black appeared uniformly opaque and matte without any iridescent color or angle dependence of the color observable by the naked eye (Figure 1b). The color was consistent throughout a sample, even though the powders prepared in this study had a wide distribution of colloidal crystal grain sizes, as shown in the SEM images (Figure 1c and d). Typical colloidal crystal grains had dimensions between a few micrometers and tens of micrometers.

Carbon black (in this case, acetylene black, prepared by thermal decomposition of acetylene), essentially consists of graphitic carbon in the form of nearly spherical, colloidal particles, coalesced into particle aggregates (23). Figure 2a shows an SEM image of the carbon black sample, in which most carbon black nanoparticles are smaller than 100 nm. Figure 2b presents an SEM image of a typical PMMA-carbon composite used in this study. The image indicates that the carbon nanoparticles do not fill the interstices and do not cover all opal domains; they are merely attached to the surface of colloidal crystal grains in limited regions. This

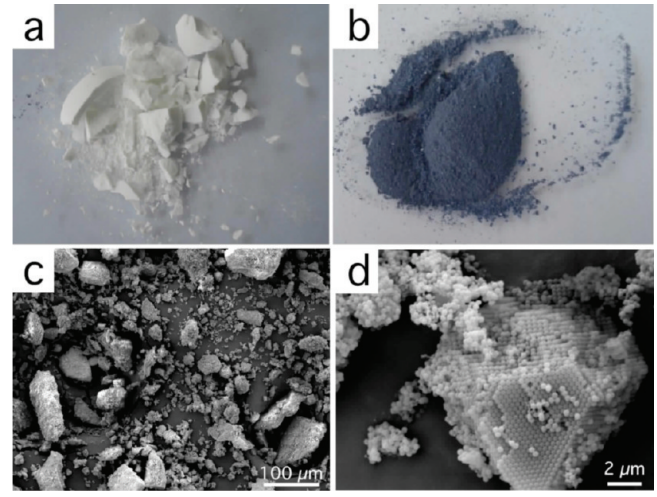

FIGURE 1. Colored powders result from mixing white PMMA colloidal crystals with small loadings of carbon nanoparticles, here producing a sample of blue color. (a) Photograph of PMMA colloidal crystal powder without carbon. (b) Photograph of powdered PMMA colloidal crystal (340 ± 10 nm spheres) with 5 wt % carbon. (c) SEM image of the blue powder after it was passed through a 200-mesh sieve. A wide distribution of colloidal crystal grain sizes is present. (d) SEM image of a grain, showing the opal structure.

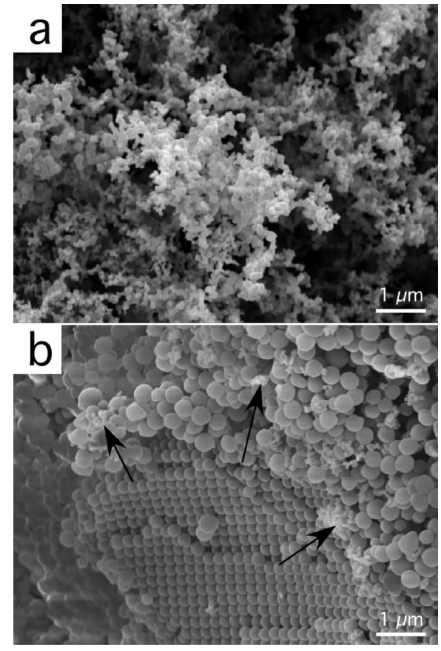

FIGURE 2. (a) SEM image of agglomerates of carbon nanoparticles. (b) SEM image of carbon particles and aggregates of such particles (see arrows) on the surface of a PMMA opal grain with polymer sphere sizes of 270 ± 10 nm. The carbon nanoparticles are significantly smaller than the polymer spheres.

situation is in contrast with the system described by Pursiainen et al., in which carbon nanoparticles are more uniformly distributed and fill interstitial sites between polymer spheres in a colloidal crystal film to enhance the color of the film (15).

Figure 3 shows UV−vis spectra and photographs of three powder samples with different colors, which depend on the different sizes of spheres composing the colloidal crystals. Several interesting features of the spectra can be noted. Each spectrum consists of a series of reflection peaks in the

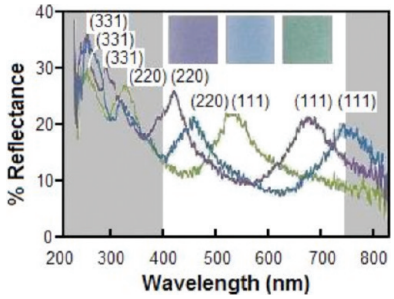

FIGURE 3. Diffuse reflectance spectra for different colored powders composed of PMMA colloidal crystals containing 5 wt % carbon black. The gray areas correspond to regions outside of the visible spectral range. The insets show photographs of the purple powder (diameter of PMMA spheres 310 ± 10 nm), blue powder (diameter of PMMA spheres 340 ± 10 nm), and green powder (diameter of PMMA spheres 240 ± 10 nm). The periodic peaks in each spectrum result from the fcc structure of the colloidal crystals. The purple sample has peaks in the violet and red spectral regions. The photos were taken using a digital camera with flash, and the sample was placed inside a black box in order to avoid reflections of ambient light. The top surfaces of the powders were leveled by tapping the samples. The insets show areas ca. 2 cm on each side.

UV−vis−IR range, associated with the periodic structure of the randomly oriented colloidal crystal particles. Sample colors arise from the sum of these peaks in the visible range. Although one might expect the order of colors to be green, blue, and then violet with decreasing sphere diameters, the observed order is blue (diameter size 340 ± 10 nm), purple (diameter size 310 ± 10 nm), and green (diameter size 240 ± 10 nm). This order arises from the fact that peaks corresponding to different sets of Miller planes appear in the visible range. For the largest spheres, the major peak is the (220) reflection at 460 nm with a small tail from the (111) reflection on the red end, and therefore the sample appears blue. The purple sample shows two peaks in the visible range, one in the violet at 418 nm (220) and one in the red region at 685 nm (111), and the color corresponds to a superposition of these reflection peaks. For the sample with the smallest sphere size, the (111) reflection at 533 nm is the only contributor to the green color of the sample. The UV−vis reflectance spectrum of carbon black by itself does not show any distinct reflection peaks that correspond to peaks in these spectra, confirming that the PMMA-carbon composite colors arose mainly from structural effects (see Supporting Information Figure S1).

Increasing the carbon content in the range from 1−8 wt % resulted in more intense coloration. Above 8 wt % or below 1 wt %, the mixtures were too dark or too white, respectively, to see well-defined colors. Within this range, however, it was possible to adjust the chromatic coordinates. Figure 4 shows photos and corresponding UV−vis spectra for a colloidal crystal sample (PMMA sphere diameter 322 ± 10 nm) without carbon and with 3 or 5 wt % carbon. The carbon-containing samples appeared increasingly darker purple as the carbon loading was increased. Notably, the spectral shapes were similar for all three samples with two broad reflection peaks around 420 and 735 nm. However, the baseline shifted to lower reflectivity as the carbon content was raised, resulting in the darker coloration.

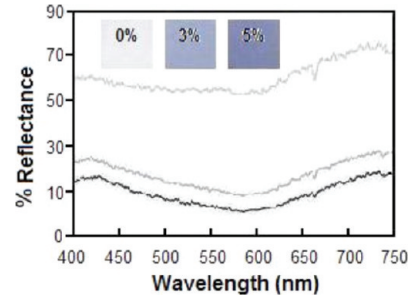

FIGURE 4. Diffuse reflectance spectra and photographs (insets) of purple PMMA opaline powders (diameter size of PMMA spheres 322 ± 10 nm) containing different amounts of carbon black. Mass percentages of carbon are indicated in the figure. The photos were taken using a digital camera with flash, inside a black box in order to avoid reflections of ambient light. The top surfaces of the powders were leveled by tapping the samples. The insets show areas ca. 2 cm on each side.

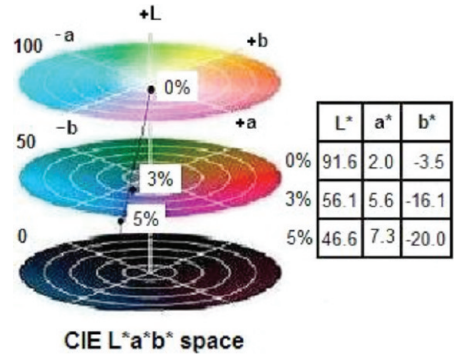

	L*	a*	b*
0%	91.6	2.0	-3.5
3%	56.1	5.6	-16.1
5%	46.6	7.3	-20.0

FIGURE 5. Color behavior of PMMA colloidal crystal powders (diameter of PMMA spheres 322 ± 10 nm) containing 0, 3, or 5 wt % carbon as indicated. Chromatic coordinates in CIE L*a*b* space.

We analyzed the color of the purple samples shown in Figure 4, using the common convention of chromatic coordinates. The Commission Internationale de l'Eclairage (CIE) accepts different models of color space, one of them being L*a*b* color space (based on nonlinearly compressed CIE XYZ color space), which identifies colors by three factors: lightness (L*), the position along the red/magenta−green axis (+a to −a), and the position along the yellow−blue axis (+b to −b). On the basis of these numbers, it is possible to reproduce similar colors of powders by using color management software, which is built into many commercial image-editing applications. The color coordinates for the purple samples containing different carbon loadings are shown in Figure 5. Varying the fraction of carbon affects all three coordinates, not only luminance. The color coordinates may also be affected by the distribution of the carbon nanoparticles. However, our experiments could not distinguish between small variations in the random distribution of carbon nanoparticles throughout the opaline powders.

Although by eye the color of the pigment powder appeared uniform regardless of viewing direction, we analyzed the angle dependence more rigorously using a paint prepared from these pigments and deposited on rigid substrates. Typical paints combine a pigment with a polymer to form a thin film and a solvent as a liquid vehicle. A challenge presented by the colloidal crystal pigments was related to their porosity. Any permanently infiltrated liquid

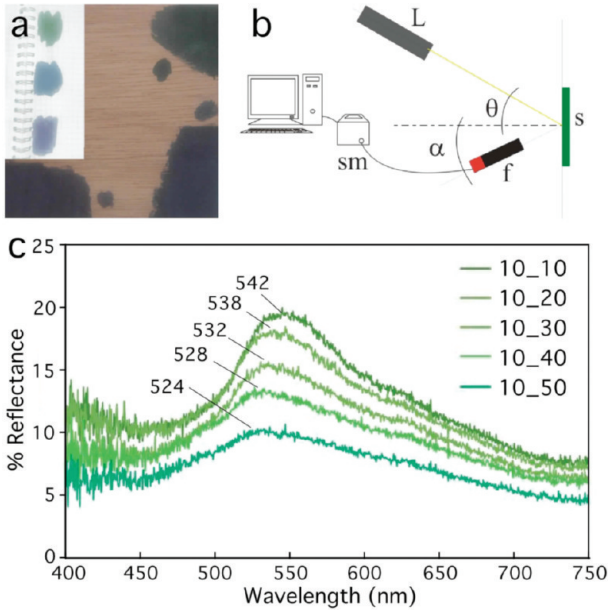

FIGURE 6. (a) Photographs of paint prepared from the colored powders in a mixture of deionized water and a solution based on polyvinyl acetate. These paints were applied on different surfaces, i.e., wood and paper (inset). (b) Experimental setup used to measure the angle dependence of the reflectance spectra with illumination at a constant angle (θ) and measurements at variable angles (α). L, halogen lamp with collimator; s, sample; sm, spectrometer; f, optical fiber probe. (c) Diffuse reflectance spectra of the paint prepared with the green powder as a function of measurement angle. The legend indicates the illumination angle (first number, always 10°) and the measurement angles (second number, from 10 to 50°). The blue shift of the diffuse reflectance peak with a higher measurement angle indicates iridescence, but iridescence was not visually observable.

within the structure can alter or destroy the color effect through refractive index matching. After testing different polymers, a commercial solution based on polyvinyl acetate mixed with deionized water was found to be suitable. The optimized composition containing 0.2 % m/v (mass of pigment and solid mass of polymer (PVA) over total volume of deionized water) was used to apply a layer on the different surfaces with a brush. Figure 6a shows examples of the dried paint applied on a piece of paper and on a piece of wood for the colored powders shown in Figure 3. The photo with paper as a substrate was taken using a camera with a flash inside a black box, and the photo with wood as a substrate was taken under diffuse natural light. The paints have a matte appearance similar to the powders. It is notable that the effective colors of the dried paint samples on white paper (Figure 6a) were virtually identical to those of the loose powders (Figure 3), indicating that PVA did not penetrate the PMMA colloidal crystals. On the darker, wooden surface, the contrast between paint and substrate was less pronounced, and the colors appeared much darker.

To analyze the angle dependence of the color, we used the setup displayed in Figure 6b, which allowed us to vary both the illumination angle (θ) and the measuring angle (α). The green paint applied on the wood surface was used for this analysis. Figure 6c shows spectra obtained at an angle of 10° for illumination and 10−50° for the measuring angle, using the notation θ_α. With increasing measuring angle,

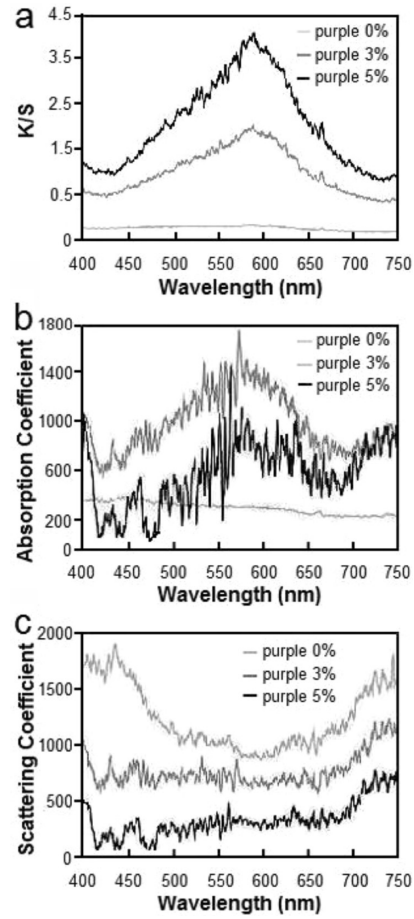

FIGURE 7. Optical behavior of PMMA colloidal crystal powders (diameter of PMMA spheres 322 ± 10 nm) containing 0, 3, or 5 wt % carbon as indicated. (a) Ratio of absorption to scattering coefficient (K/S) as a function of wavelength. (b) Absorption coefficient as a function of wavelength ($K(\lambda)$). (c) Scattering coefficient as a function of wavelength ($S(\lambda)$).

the (111) peak gradually shifted to the blue from 542 nm (10_10) to 524 nm (10_50), i.e., by 18 nm over 40°. The behavior was similar for sets of spectra obtained at different angles of illumination. This angular dependence of the *spectra* is significantly less than what was observed for liquid membranes with structural colors (12). Similar to the current systems under examination, these liquid membranes showed little angle dependence to the *eye*.

The appearance of these structural composite pigments is affected by both absorption and scattering of incident light. This behavior may be modeled by the Kubelka−Munk theory, which relates the ratio of absorption (K) and scattering (S) to reflectance of an infinitely thick layer (R_∞; we used 5-mm-thick layers to determine R_∞) at a given wavelength (eq 1).

$$\frac{K}{S} = \frac{(1 - R_\infty)^2}{2R_\infty} \qquad (1)$$

Figure 7a shows the K/S curves obtained after application of eq 1 to the spectra in Figure 4.

In order to separate the absorption and scattering components, we then applied a controlled thick layer (h = 100

μm) of paint over a rigid dark substrate (exposed photo paper for black and white photography) and measured spectra of pigment layers with different carbon contents (R). We used the spectrum of the rigid dark substrate (R_0) and the reflectance spectrum of the "infinitely thick" layer of pigment (R_∞) for calculating the constants a and b in eq 2, which were then employed in eq 3 to calculate separate K and S values at each wavelength (24). Results are shown in Figure 7b and c. The correctness of the absorption and scattering curves was verified by taking the ratio of the two curves and recovering the K/S curves in Figure 7a.

$$a = \frac{1}{2}\left(\frac{1}{R_\infty} + R_\infty\right) \quad b = a - R_\infty \tag{2}$$

$$S = \frac{1}{bh}\mathrm{arcoth}\left(\frac{1 - a(R + R_0) + RR_0}{b(R - R_0)}\right) \quad K = S(a - 1) \tag{3}$$

When the sample does not contain any carbon, scattering predominates, absorption is very low, and the curve of the absorption coefficient as a function of wavelength ($K(\lambda)$) is flat. Increasing the carbon content of the samples disturbs this behavior with less absorption in the violet and red regions of the spectrum where reflection peaks were observed and maximum absorption in the broad range in between. For the scattering coefficient as a function of wavelength ($S(\lambda)$), the curve of the carbon-free sample follows the form of the reflectance spectrum in Figure 4, and scattering intensities decrease with higher carbon content.

On the basis of these data, we propose the following qualitative explanation for the matte, uniform color and absence of iridescence in these structural pigments. Let us consider an ideal photonic crystal, which allows certain wavelengths to pass through and rejects other wavelengths (Figure 8a). Scattering by opaline domains in multiple directions generates the white appearance (Figure 8b). If a photonic crystal is in contact with a dark surface, the rejected color appears stronger than the other colors due to enhanced absorption of the transmitted wavelengths (Figure 8c). The colored powders contain randomly sized and oriented domains of opals (typically some tens of micrometers in diameter), including both ordered and disordered domains with attached carbon nanoparticles. The domains behave as "photonic particles" (with pseudo-PBG), which scatter and reflect light differently compared to regular pigments without structural color. The domain sizes are important because they affect the mean free path of the light, the efficiency of reflection, and scattering among multiple domains (25, 26). In the PMMA-carbon composites, the carbon nanoparticles generate extinction, which results from both absorption and Rayleigh scattering. Therefore, in the composite particles, all wavelengths are absorbed except those in the pseudo-PBG, which are reflected in many directions, leading to the uniform appearance of the sample with little iridescence (Figure 8d). A more complete, quantitative model of the color effects would require the use of the scattering matrix method (27) and extended kinematic diffraction theory (28), which takes into account the transmission, reflection, and diffraction by the crystalline colloidal arrays.

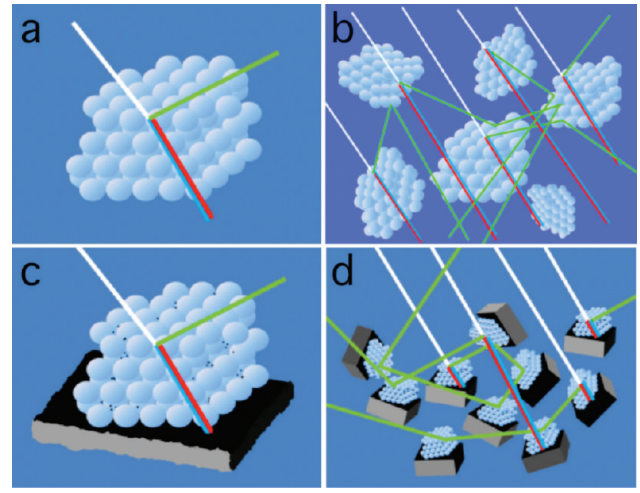

FIGURE 8. Qualitative explanation of the proposed coloration mechanism. (a) A highly crystalline polymer opal transmits light of some wavelengths and reflects other wavelengths. This response is angle-dependent, resulting in an opalescent appearance. (b) Smaller opal domains scatter light, generating the white appearance of opaline powders. (c) If the polymer opal is placed on a dark surface, transmitted light is absorbed, and the reflected light is more visible. (d) Many randomly oriented opaline domains in contact with a dark surface scatter the predominant wavelength of the pseudo-photonic band gap. For easier visualization, the size of the dark surfaces is exaggerated in this schematic diagram compared to the powdered samples discussed in this paper. However, similar color effects can be observed if the opaline powders are rubbed onto a dark surface (see the Supporting Information, Figure S2).

CONCLUSION

Whereas traditional pigments obtain their coloration through different methods of selective absorption (29), the phenomena discussed here open the possibility of achieving uniform coloration by a material with an ordered-disordered structure, which combines a pseudo-PBG effect (order) with scattering and absorption processes (disorder). Colored powders without iridescence were obtained by mixing PMMA opals with small fractions of carbon nanoparticles, both materials that by themselves do not absorb selectively in the visible range. The structural color was determined largely by the PMMA sphere sizes, and the lightness of the colors could be adjusted by changing the fraction of carbon black in contact with the colloidal crystals. These colored powders are good candidates as new light-stable pigments that can be readily prepared by scalable processes. Because these pigments rely on light reflection, their colors are best defined under intense light, such as sunlight or the light of a camera flash. Under low intensity light, the colors are less well pronounced.

A basic paint was prepared by a combination of the colored powders with a commercial mixture of polyvinyl acetate as a binder and deionized water as the solvent, which was applied on several kinds of surfaces and maintained the color of the powders after drying. Spectral analysis of these paints revealed only a very small angle dependence of the

main reflection peak. Application of Kubelka–Munk theory showed that scattering is the predominant factor influencing the reflection of the pigments at very low carbon contents, but absorption becomes more important as the carbon loading increases in the range from 1–8 wt %. A proposed mechanism of the coloration depends on incomplete PBGs of the PMMA colloidal crystal particles, good contact between these and the carbon nanoparticles that absorb and scatter light, as well as on random sizes and orientations of the colloidal crystal domains.

Acknowledgment. C.I.A. and E.R. thank CONACYT (Mexico) for financial support. A.S. acknowledges partial funding of this work by the National Science Foundation (DMR-0704312) and by the U.S. Department of Energy (DE-FG02-06ER46348). Parts of this work were carried out at the University of Minnesota Characterization Facility, which receives partial funding from the NSF through the MRSEC and NNIN programs.

Supporting Information Available: UV–visible reflectance spectrum of the carbon black powder and photograph of PMMA colloidal crystal powders spread on a dark surface. This material is available free of charge via the Internet at http://pubs.acs.org.

REFERENCES AND NOTES

(1) Yablonovitch, E. *Phys. Rev. Lett.* **1987**, *58*, 2059.
(2) John, S. *Phys. Rev. Lett.* **1987**, *58*, 2486.
(3) Joannopoulos, J. D.; Johnson, S. G.; Winn, J. N.; Meade, R. D. *Photonic Crystals: Molding the Flow of Light*, 2nd ed.; Princeton University Press: Princeton, NJ, 2008.
(4) Prather, D. W.; Shi, S.; Sharkawy, A.; Murakoswki, J.; Schneider, G. J. *Photonic Crystals, Theory, Applications, and Fabrication*; Wiley: Hoboken, NJ, 2009.
(5) López, C. *Adv. Mater.* **2003**, *15*, 1679.
(6) Blanford, C. F.; Schroden, R. C.; Al-Daous, M.; Stein, A. *Adv. Mater.* **2001**, *13*, 26.
(7) Blanford, C. F.; Yan, H.; Schroden, R. C.; Al-Daous, M.; Stein, A. *Adv. Mater.* **2001**, *13*, 401.
(8) Schroden, R. C.; Al-Daous, M.; Blanford, C. F.; Stein, A. *Chem. Mater.* **2002**, *14*, 3305.
(9) Velev, O. D.; Lenhoff, A. M.; Kaler, E. W. *Science* **2000**, *287*, 2240.
(10) Yu, Z. Y.; Chen, L.; Chen, S. *J. Mater. Chem.* **2010**, *20*, 6182.
(11) Kim, S.-H.; Jeon, S.-J.; Yang, S.-M. *J. Am. Chem. Soc.* **2008**, *130*, 6040.
(12) Rodriguez-Moraz, S. l.; Albrecht, T.; Anselmann, R. Pigments. Canadian Patent 2408990, Nov 15, 2002.
(13) Munro, C.; Merritt, M. D.; Lamers, P. H. Color effect compositions. U.S. Patent 6,894,086 B2, May 17, 2005.
(14) Wulf, M.; Taennert, K.; Allard, D.; Zentel, R. Process of Preparation of Specific Color Effect Pigments, International Patent WO/2006/116640, Nov 2, 2006.
(15) Takeoka, Y.; Honda, M.; Seki, T.; Ishii, M.; Nakamura, H. *ACS Appl. Mater. Interfaces* **2009**, *1*, 982.
(16) Harun-Ur-Rashid, M.; Imran, A. B.; Seki, T.; Ishii, M.; Nakamura, H.; Takeoka, Y. *ChemPhysChem* **2010**, *11*, 579.
(17) Müller, M.; Zentel, R.; Maka, T.; Romanov, S. G.; Sotomayor-Torres, C. M. *Adv. Mater.* **2000**, *12*, 1499.
(18) Donnet, J.-B.; Bansal, R. C.; Wang, M.-J. *Carbon black*, 2nd ed.; Marcel Dekker Inc.: New York, 1993.
(19) Pursiainen, O. L. J.; Baumberg, J. J.; Winkler, H.; Viel, B.; Spahn, P.; Ruhl, T. *Opt. Express* **2007**, *15*, 9553.
(20) Wang, X. H.; Akahane, T.; Orikasa, H.; Kyotani, T. *Appl. Phys. Lett.* **2007**, *91*, 011908.
(21) Gutcho, M. H. *Inorganic Pigments: Manufacturing Processes*; Noyes Data Corp.: Park Ridge, NJ, 1980; p 187.
(22) Xia, Y.; Gates, B.; Yin, Y.; Lu, Y. *Adv. Mater.* **2000**, *12*, 693.
(23) Patton, T. C. *Pigment Handbook*; Wiley: New York, 1973; Vol. I.
(24) Völz, H. G. *Industrial Color Testing. Fundamentals and Techniques*, 2nd ed.; Wiley-VCH: Weinheim, Germany, 1995.
(25) Ishimaru, A. *Wave Propagation and Scattering in Random Media*; IEEE Press Oxford University Press: New York, 1997.
(26) Koenderink, A. F.; Vos, W. L. *J. Opt. Soc. Am. B* **2005**, *22*, 1075.
(27) Balestreri, A.; Andreani, C.; Agio, M. *Phys. Rev. E* **2006**, *74*, 036603.
(28) Tikhonov, A.; Coalson, R. D.; Asher, S. *Phys. Rev. B* **2008**, *77*, 235404.
(29) Nassau, K. *The Physics and Chemistry of Color*, 2nd ed.; John Wiley & Sons Inc.: New York, 2001.

AM100704F